The Role of Thickness Transitions in Convective Assembly

Linli Meng, Hong Wei, Anthony Nagel, Benjamin J. Wiley, L. E. Scriven and David J. Norris[*]

Department of Chemical Engineering & Materials Science,

University of Minnesota, 421 Washington Avenue SE, Minneapolis, MN 55455 USA

[*]Corresponding author. E-mail: dnorris@umn.edu

Supporting Information

Nitrogen Delivery System. To control the evaporation rate from our growth cells (depicted in Fig. 1), a simple flow system was constructed to achieve uniform delivery of dry nitrogen gas. A cylindrical metal tube, ~4cm in diameter and ~15 cm in length, was used as a reservoir. Nitrogen gas (ultra high purity grade) was fed into the flat end of the cylinder. This entrance port was offset from the center of the tube to aid in mixing. The nitrogen then exited the tube via a slot in the curved face at the center of the tube. Two parallel metal plates were inserted into this slot and directed the nitrogen toward the cell. These plates formed a narrow channel 15 cm long (radiating away from the tube), 2.5 cm wide (to match the width of the cell), and 0.64 mm high. The metal plates were assembled by screws and adjusted with shims to ensure that they were parallel. The geometry of the plates (long with a narrow spacing) was chosen to obtain a laminar flow with a spatially uniform flow rate at the exit of the slot. The exit of the slot was positioned at the top of the inclined cell wall (where the crystal deposited). The

flow was directed 20° from horizontal (downward toward the cell). The typical flow rate was 2.4 L/minute.

SUPPORTING FIGURE CAPTIONS

Figure S1. Detailed assembly steps. Using the simple geometric model, described in the text, convective assembly was simulated through the bilayer to trilayer transition. For each step of the process (1-20), the top view and cross-section are shown. To obtain the structures in 3, 7, 12, and 16, the sphere positions are "relaxed" to achieve close-packing while transitioning gradually from hexagonal to square and then back to hexagonal packing. In steps 2, 4-6, 9-11, 13-15, and 17-19, a row of spheres is added to the structure. The position of attachment is governed by the assumption that the growth front must maintain a "ramp" shape. Note that for step 2, the new row of spheres can attach at two positions (denoted 2a and 2b). However, both lead to the structure shown in 3 when the structural relaxation occurs. Finally, between 7 and 8 the structure propagates by adding three more rows of square packed spheres. The structure can propagate like this indefinitely before transitioning to three hexagonally packed layers. Between 19 and 20, the structure propagates by adding three more rows of hexagonally packed spheres. This would continue until a transition from the trilayer to the 4-layer occurs.

Figure S2. Trilayer to 4-layer transition. (a) and (b) Simulated structure (top view and cross-section, respectively) predicted by our simple geometric model. A series of steps, similar to those shown in Fig. S1, leads to this structure. The trilayer of hexagonally packed spheres is at the top of the image; the 4-layer is at the bottom. The transition initiates a very specific stacking sequence in the 4-layer (*ABAC*, listed from the substrate to the top). Note that the facet exposed at the bottom of the simulations does not represent the expected growth front, but rather was chosen to clearly see the *ABAC* stacking sequence. (c) Confocal microscopy images of a transition region with *ABAC* stacking, obtained by infiltrating the crystal with a solution of fluorescent dye. The images are inverted such that "white" indicates the absence of fluorescent dye. The 4th (furthest from the substrate), 3rd, 2nd, and 1st layers

are shown from left to right. 40% of the trilayer to 4-layer transition regions which were probed had this sequence. (d) and (e) Simulated structure (top view and cross-section, respectively) obtained by slight modifications of the assembly steps used in (a) and (b). In this case, the transition forms *ABCB*. Note that the facet exposed at the bottom of the simulations does not represent the expected growth front, but rather was chosen to clearly see the *ABCB* stacking sequence. (f) Confocal microscopy images as in (c) for a sample with the *ABCB* sequence. The 4th (furthest from the substrate), 3rd, 2nd, and 1st layers are shown from left to right. 30% of the trilayer to 4-layer samples which were probed had this sequence.

MOVIE CAPTIONS

Movie 1. Real-time video recording of convective assembly. Steady-state growth (*i.e.*, without a thickness increase) of 4-layers of 1μm silica spheres is observed for a substrate inclined 45 degrees from vertical (see Fig. 1). The contrast of the images were enhanced to better visualize the particles. Note that the crystal is depositing on the other side of the transparent substrate. Gravity is pointing downward in the frame.

Movie 2. Real-time video recording of the initial stages of the crystal growth. Before convective assembly begins, the solvent wets the substrate up to the contact line, observed as a faint line sloping from the upper right corner of the frame downward to the left. A row of spheres (1μm silica) lodges near the contact line and then convective assembly of the monolayer begins. Similar effects have been reported previously (*e.g.*, see Refs. 19 and 43). Gravity is pointing downward in the frame and the substrate was inclined at 50 degrees from vertical.

Movie 3. Real-time video recording showing structural transitions occurring in the packing. At the top of the frame is a monolayer. The crystal has already transitioned to a bilayer and then during the recording it transitions to a trilayer. Transition regions are denoted by square packed arrangements of spheres. The spheres in the transition region are observed to be shifting between hexagonal packing and square packing along the growth front. These shifts appear to be initiated by changes in the

thickness of the wedge-like layer underneath the gas-liquid interface (see text for additional discussion). While our simple geometric model allows us to make clear predictions about the expected structure, this recording also shows that the actual growth is more complicated than our model. Many structural changes are occurring simultaneously in contrast to our assumption of a step by step process (see Fig. S1). Gravity is pointing downward in the frame, 1μm silica spheres were used, and the substrate was inclined at 50 degrees from vertical. See also footnote 49 in text.

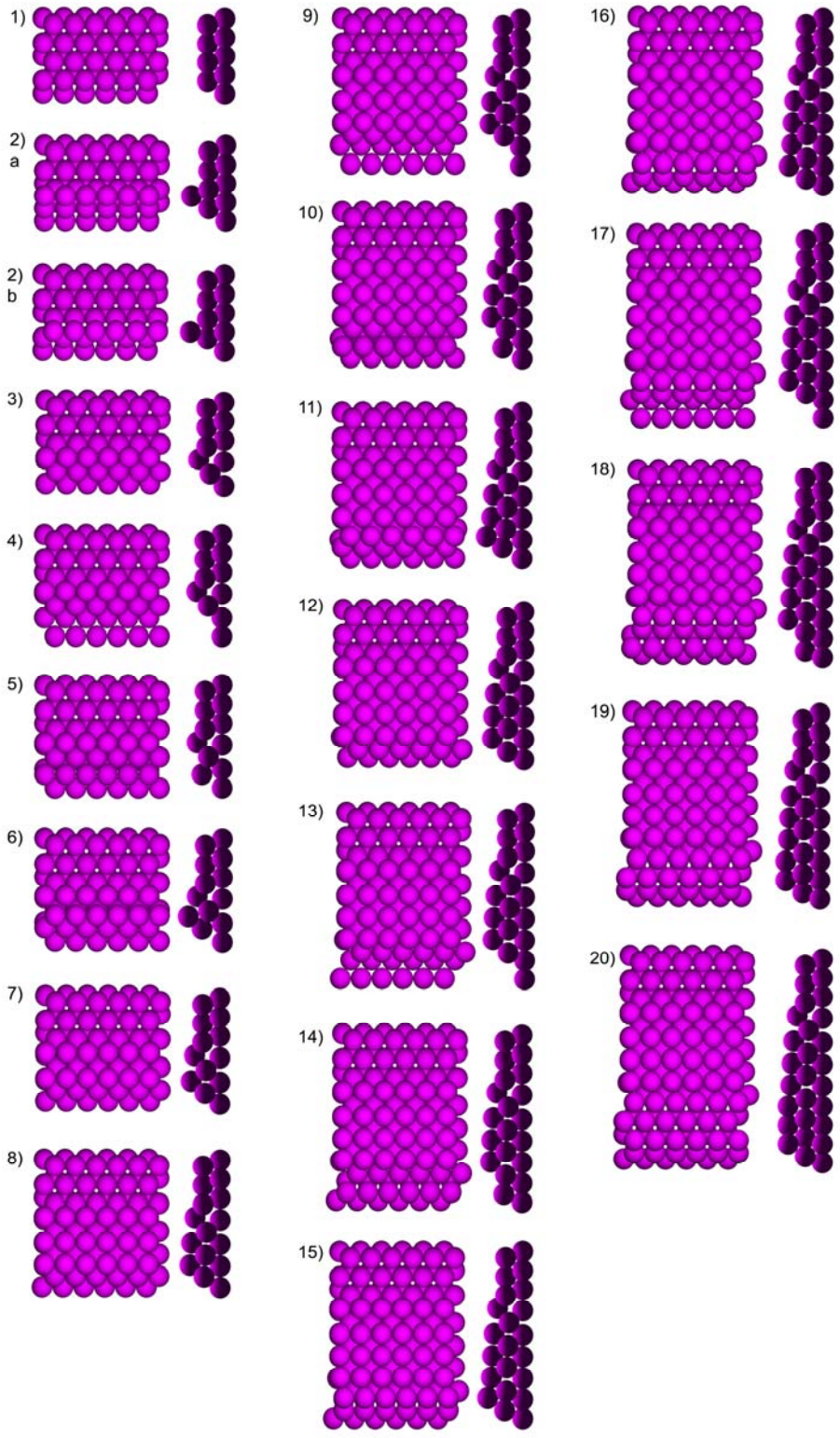

Figure S1

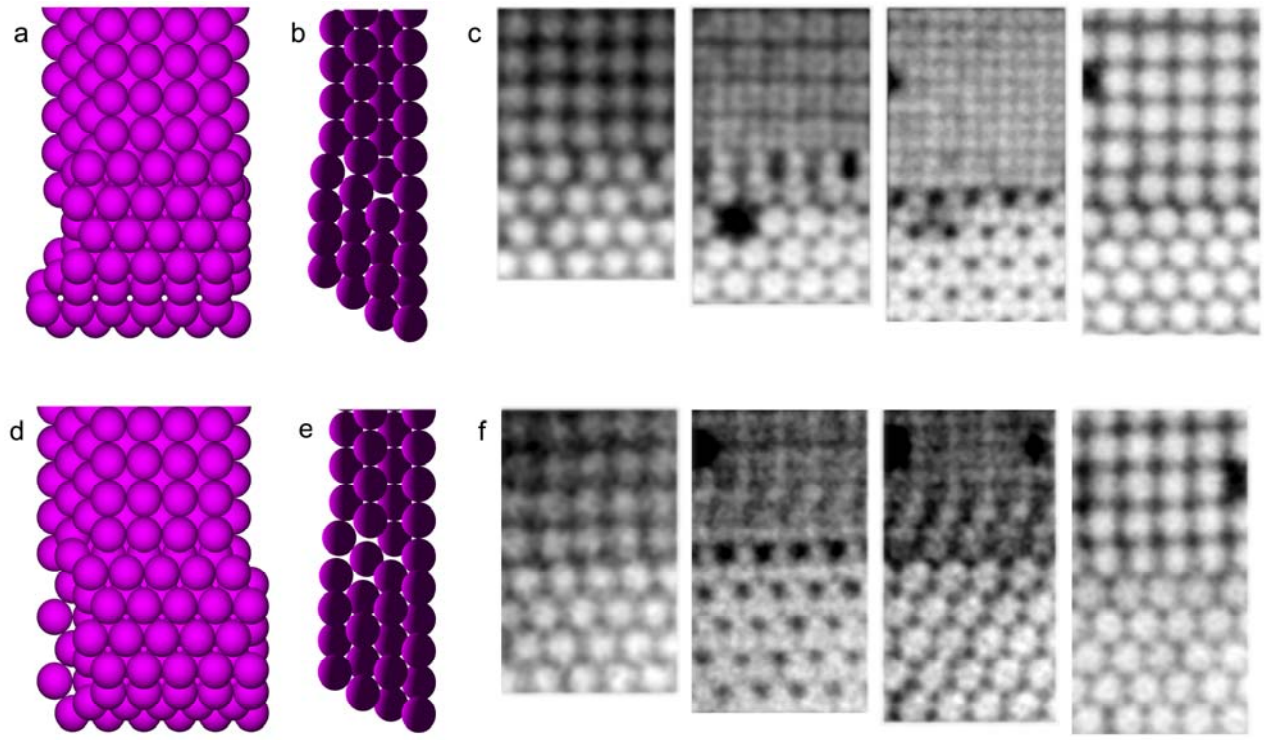

Figure S2